



Shaking Table Test of a Bridge Model Installed DRF-Dampers

A. Yamasaki⁽¹⁾, M. Hada⁽²⁾, S. Ushijima⁽³⁾, T. Matsubara⁽⁴⁾ and K. Yamamoto⁽⁵⁾

⁽¹⁾ Research Engineer, Asunaro Aoki Construction Co., Ltd, Japan, akira.yamasaki@aaconst.co.jp

⁽²⁾ Research Engineer, Asunaro Aoki Construction Co., Ltd, Japan, masaya.hada@aaconst.co.jp

⁽³⁾ Director of Institute of Technology, Asunaro Aoki Construction Co., Ltd, Japan, sakae.ushijima@aaconst.co.jp

⁽⁴⁾ Deputy Manager, Metropolitan Expressway Co., Ltd, Japan, t.matsubara813@shutoko.jp

⁽⁵⁾ Chief, Metropolitan Expressway Co., Ltd, Japan, k.yamamoto576@shutoko.jp

Abstract

It has recently been required that road bridges keep functioning immediately for a level-2 earthquake (as defined by the Japan Society of Civil Engineers). However, when bridge pier bases plasticize, it is not easy to grasp the degree of damage and repair damage. In addition, restoration ability such as quick inspection and repair work after the earthquake may not be sufficient. Furthermore, in the case of existing bridges that are not considered Level-2 earthquake at design, damage may be transferred to bottom plate and foundation of bridge pier, which are difficult to inspect and repair. Therefore, in the bridges axial direction, replacing bearing, changing to horizontal force dispersion structure during earthquake, and installing various seismic control devices are increasing. However, if seismic control devices with the velocity dependent viscous damping mechanism are used in the direction perpendicular to the bridges axis, bearing displacement (relative displacement of the superstructure and the top of substructure) also occurs at the level-1 earthquake. Therefore, it is necessary to replace an expansion device that can follow the displacement in that direction, and seismic reinforcement using seismic control devices is not widely used. Then, the authors developed a method for seismically retrofitting for the direction perpendicular to the bridge axis of existing road bridges using “Die and rod friction dampers (hereinafter referred to as DRF-dampers)”.

The DRF-damper uses the friction between metal parts known as die and rod. DRF-dampers are not displaced under the designated load. If the designated load is reached, DRF-dampers are displaced with constant frictional force. This is known as the rigid-plastic hysteretic characteristic. The proposed method uses the rigid-plastic hysteresis characteristic of the DRF-dampers. The DRF-dampers doesn't slide during a level-1 earthquake. Therefore, the DRF-dampers acts as a substitute for the side block which restrain bearing displacement. On the other hands, the DRF-dampers slides during a level-2 earthquake. As a result, the DRF-dampers sets a limit to the inertia force of the superstructure. And more, the DRF-dampers absorb seismic energy efficiently to reduce the response of the substructure.

This paper shows the outline of the proposed method. And, we made a bridge model installed the DRF-dampers (photo 1) and describe the result of the shaking table test reproducing the dynamic behavior at the time of earthquake in this paper. As a result of the experiment, reinforcement using the DRF-dampers was able to reduce the response value of the bridge substructure at the level-2 earthquake by about 60% as compared with before reinforcement.

Keywords: Friction dampers, Die-and-rod, Bridge, Seismic control, Seismic retrofit



Photo 1 – Shaking table test situation



1. Introduction

Japanese road bridges may be required to function as an evacuation route or as a transportation route for emergency supplies immediately after a Level 2 earthquake. Therefore, maintaining functions immediately after the earthquake has become an issue. Since 1996, to plasticize bridge pier bases, measures have been taken the steel plate winding to bridges pier, and, exchanging to bearing that have load bearing capacity than horizontal load bearing capacity of bridge pier. However, when bridge pier bases plasticize, it is not easy to grasp the degree of damage and repair. Also, from the viewpoint of restoration ability, there is a risk that a quick inspection and repair may be inadequate. In addition, in the case of an existing bridge that has not been designed in consideration of a level-2 earthquake, the damage may shift to the bottom plate or the base of the bridge pier. For this reason, in the bridges axial direction, isolation by support replacement, changing to horizontal force dispersion structure during earthquake, and using various seismic control devices are increasing [1]. However, if seismic control devices with the velocity dependent viscous damping mechanism are used in the direction perpendicular to the bridges axis, support displacement also occurs at the level-1 earthquake. Therefore, it is necessary to replace it with a joint that can follow the displacement in that direction, and seismic reinforcement using seismic control devices is not widely used.

Accordingly, the authors developed a method for seismically retrofitting for the direction perpendicular to the bridge axis of existing road bridges using “Die and rod friction dampers (hereinafter referred to as DRF-dampers)” (Fig. 1) [2][3][4][5].

This paper shows the outline of the proposed method. And, we made a bridge model installed the DRF-dampers and describe the result of the shaking table test reproducing the dynamic behavior at the time of earthquake [6][7].

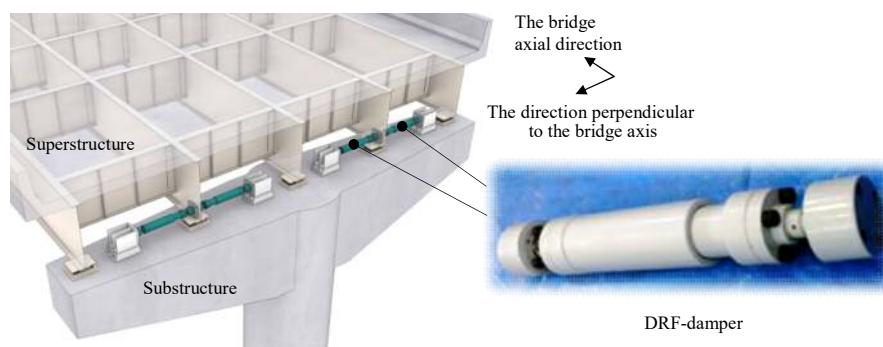


Fig. 1 – Method of seismically reinforcing a bridge which uses friction dampers

2. A method for seismically retrofitting using DRF-dampers

2.1 Outline of a DRF-damper

A DRF-damper is a damper which utilizes friction between metal parts called a die and rod. A DRF-damper is already being used for seismic reinforcement of building structures [8]. DRF-dampers are not displaced under the designated load. If the designated load is reached, DRF-dampers are displaced with constant frictional force. This is known as the rigid-plastic hysteretic characteristic (Fig. 2).

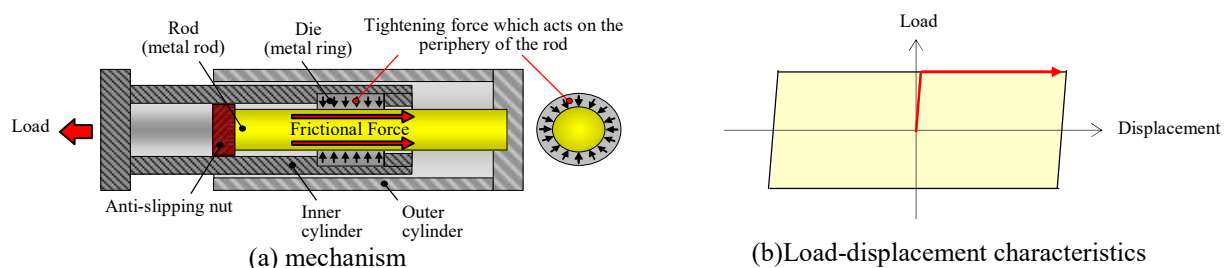


Fig.2 – Outline of DRF-damper



2.2 Effectiveness of seismic control using this method

The proposed method uses the rigid-plastic hysteresis characteristic of the DRF-dampers (Fig. 3). The DRF-dampers doesn't slide during a level-1 earthquake. Therefore, the DRF-dampers acts as a substitute for the side block which restrain bearing displacement (Fig. 3 (a),(b) Left). On the other hands, the DRF-dampers slides during a level-2 earthquake. As a result, the DRF-dampers sets a limit to the inertia force of the superstructure. And more, the DRF-dampers absorb seismic energy efficiently to reduce the response of the substructure (Fig. 3 (a),(b) Right). According to published data [2], time history response analysis was carried out on an RC single column bridge pier. As a result, by using this method to perform seismic reinforcement, it is confirmed that the damage (degree of curvature) sustained by the bridge pier base can reduce to one half of the damage sustained before reinforcement. Also, a high-speed shaking test was performed on a DRF-damper which had increased capacity for using to bridges. As a result, it was found that even if under a high shaking amplitude exceeding 10 cm and also high-speed shaking exceeding 100 cm/sec, the DRF-damper exhibits the predicted energy absorption performance.

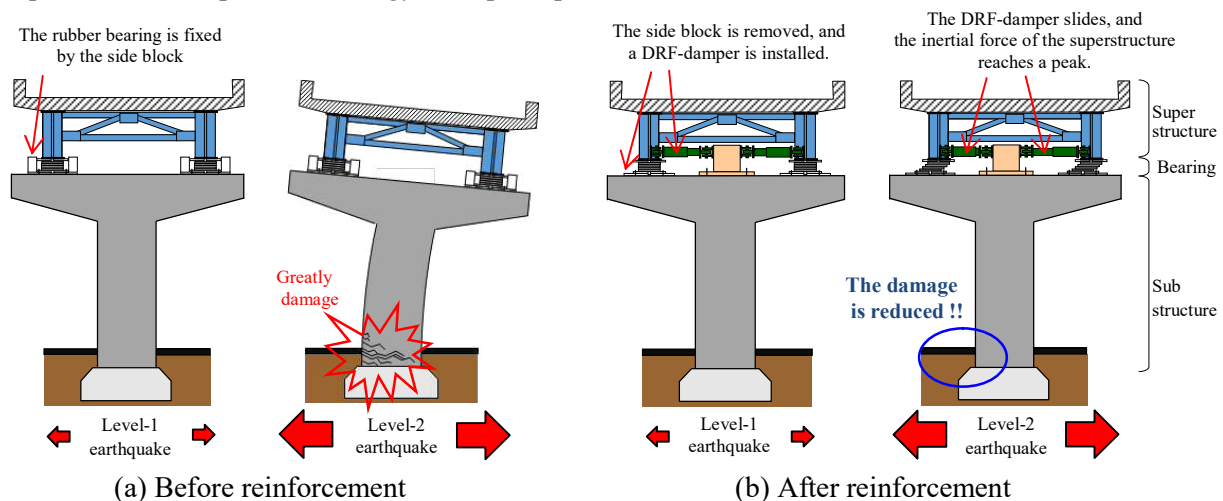


Fig.3 – Conceptual drawing showing the effectiveness of seismic control using this method

3. The outline of the shaking table test

3.1 Test model

The exterior perspective used as the test model is shown in Fig. 4. The installation condition of the DRF-damper is shown in Photo.1, and the installation condition of the upper and lower rubber bearing is shown in Photo. 2. In addition, Table 1 shows a comparison between the specifications of the test model and the specifications of an actual bridge. The test model is modeled RC single column bridge piers of an actual bridge by two-quality point model. The upper and lower levels of the test model correspond to the superstructure and the substructure of an actual bridge. The specifications of the test model were set based on the rules of similarity shown in Table 1. The similarity index for the acceleration of the test model is 1.0 to an actual bridge, the index of similarity for length is 1/2.22 and the time is 1/1.49. The upper frame including the counterweight had a total weight of 507 kN, and the upper rubber bearing supported the upper frame to set the same support conditions as an actual bridge. Also, the elastic spring stiffness of the lower rubber bearing reproduced the shear stiffness of the substructure. There are a total of four DRF-dampers consisting of two each in the north and south faces between the upper and lower levels. They are installed parallel to the upper rubber bearing. The ends of each DRF-damper are connected by pins: One end is pinned to the upper frame, and the other end is pinned to the lower frame. In this test, the stipulated acceleration waveform was input to the shaking table, the test model was acted an inertial force (mass \times acceleration) (Fig. 5). The acceleration was measured at the center part of each of the upper and lower frames, and the interlayer displacement was measured using a displacement gauge installed between layers. Also, the reaction force of the bearing was measured using a tridirectional power gauge installed directly beneath the upper and lower



rubber bearing. The acceleration waveform was input to east-west direction (direction perpendicular to the bridge axis) which is the direction of the DRF-damper was installed. The positive direction defined the west-facing direction. As a result of performing sweep wave shaking in advance, the primary natural frequency of the test model without the DRF-damper (rubber bearing only) was 0.68 sec, and the attenuation constant (estimated using the 1/2 method) was 6.4 %.

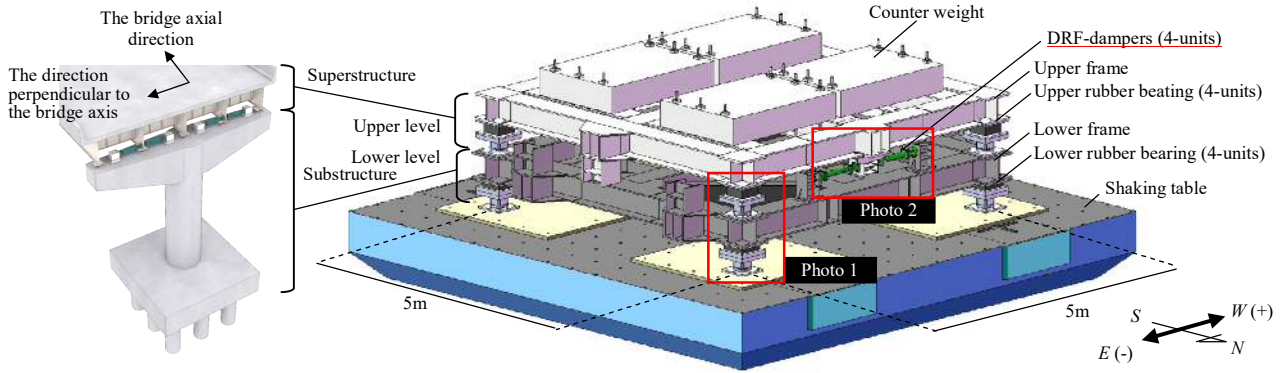


Fig. 4 – External perspective of the test model

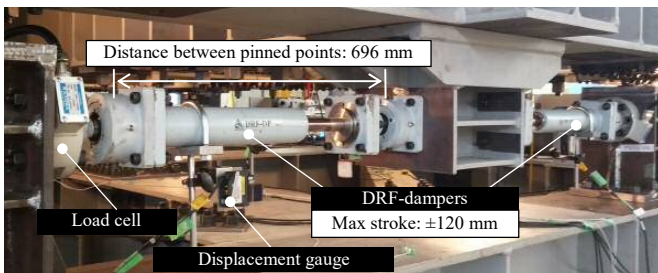


Photo 1 – Installation situation of the DRF-damper

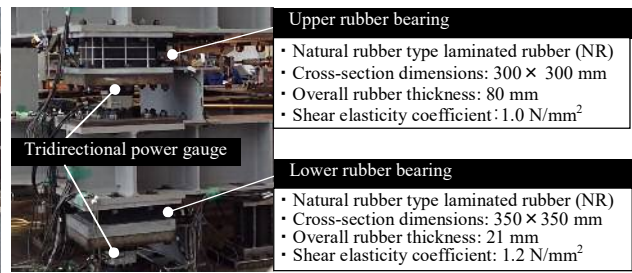


Photo 2 – Upper and lower rubber bearings

Table 1 – Specifications of the test model

Item	Unit	Actual bridge (Per bridge pier)	Test model	Similarity index
Upper (superstructure) weight	kN	5548	507	1/α ³
Upper bearing shear stiffness	kN/mm	-	4.7	-
Lower (substructure) weight	kN	-	94	-
Lower bearing shear stiffness	kN/mm	-	26.0	-
Primary natural frequency	sec	1.07	0.72	1/√α
Lower yield resistance	kN	5167	(472)	1/α ³
Displacement	mm	1	1/2.22	1/α
Velocity	cm/sec	1	1/1.49	1/√α
Acceleration	cm/sec ²	1	1	1/1.0
Time	sec	1	1/1.49	1/√α

※1: The similarity index is expressed by the test model/actual bridges, and the scale index α is deemed to be 2.22.

※2: The lower yield resistance of the test model is a value assumed from an actual bridge, based on similarity rules.

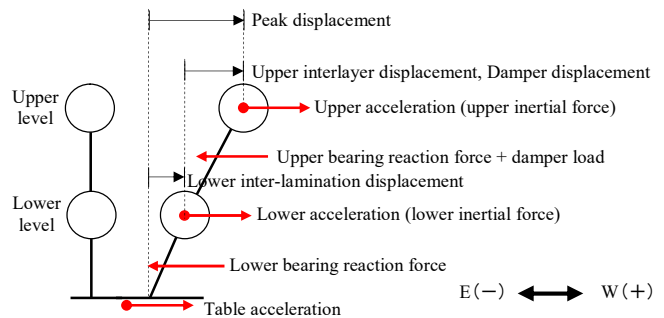


Fig. 5 – Conceptual drawing of measurement items

3.2 Shaking Cases

The test body setup is shown in Fig. 6, and a list of shaking cases is shown in Table 2. The shaking cases were classified as Case1 to Case4 which differ in respect of the support conditions in the direction perpendicular to bridge axis of the upper. The support condition is whether or not a DRF-damper is installed, and whether or not change the damper load. Here, the value obtained by dividing the damper load by the upper overall weight of 507 kN is defined as the damper load coefficient β. Case1 is the case of a fixed bearing condition, in which upper interlayer displacement fails to occur because of the unification of the upper and lower levels using the fixing jig. In this case, the damper load is deemed to be infinite (β = ∞) (Fig.



(a). Case2 and Case3 are cases in which the fixing jig has been removed, and the DRF-damper is installed parallel to the upper rubber bearing (Fig. (b)). The damper load values set to 200 kN ($\beta = 0.4$) and 100 kN ($\beta = 0.2$) respectively. The DRF-damper was set so that it functioned as an attenuation member from an upper acceleration of approximately 200 to 400 cm/sec². Case4 is the case where both the fixing jig and the DRF-damper are removed, and the direction perpendicular to the bridge pier is supported by the upper rubber bearing only. In this case, the damper load is deemed to be 0 kN ($\beta = 0$). (Fig. (c)).

Generally, in the case of the direction perpendicular to the axis of an existing bridge, there is no need to take into account thermal expansion and contraction of the superstructure. Also, in order to avoid damage to superstructure connecting members, side blocks are installed, resulting in fixed bearing conditions (equivalent to Case1). However, under the fixed bearing conditions, in the case of a level-2 earthquake an excessively reaction force will act on the bridge pier base, making it impossible to avoid a greatly plasticization. In this method, first the side block is removed (equivalent to Case4), and in addition the DRF-damper is installed, aiming at reducing the response value on the substructure (equivalent to Case2 and Case3).

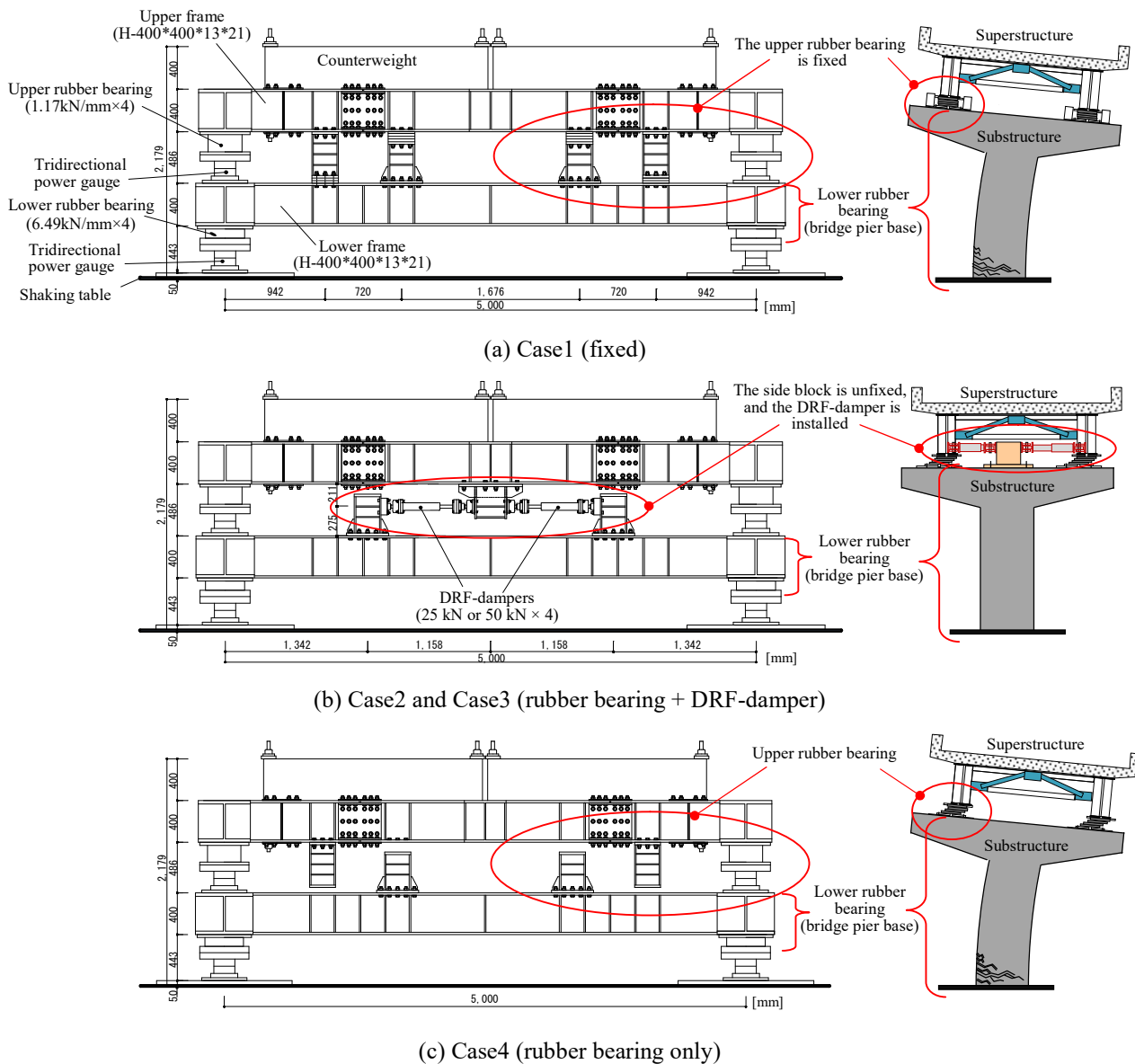


Fig. 6 – Test body setup (east-west face)



Table 2 – List of shaking cases (Case1 to Case4)

Shaking cases	Conditions for supporting the upper frame in the direction perpendicular to the bridge axis	Set value of the damper load coefficient β	Description	Remarks
1	Fixed	$\beta = \infty$	This case uses the fixing jig to unify the upper level with the lower level. It corresponds to the fixed bearing conditions which prevent upper level interlayer displacement from occurring. In this case, the damper load is set to infinity.	Before reinforcement
2	Rubber bearing + 200 kN DRF-damper	$\beta = 0.4$	In this case, the damper load of 200 kN ($50 \text{ kN} \times 4 = 200 \text{ kN}$) is installed parallel to the rubber bearing.	After reinforcement
3	Rubber bearing + 100 kN DRF-damper	$\beta = 0.2$	In this case, the damper load of 100 kN ($25 \text{ kN} \times 4 = 100 \text{ kN}$) is installed parallel to the rubber bearing.	After reinforcement
4	Rubber bearing only	$\beta = 0$	In this case, both the fixing jig and the DRF-damper are removed, so that the horizontal direction is supported by the rubber bearing only. This case is implemented to obtain a grasp of the relationship between the magnitude of the damper load and the maximum response value.	—

* The load coefficient β is the non-dimensional value of the damper reaction divided by 507 kN.

3.3 Input waveform specifications

The specifications of the input waveform are shown in Table 3, and the acceleration response spectrum is shown in Fig. 7. A waveform whose time axis was corrected in accordance with the abovementioned similarity rule to the design seismic shaking indicated in “Road bridge specifications V” was used as the input waveform [9]. In the case of a level-1 earthquake, it verifies that the DRF-damper functions as a fixed member. Therefore type III ground which has the highest acceleration at type I to III ground was selected. In the case of a level-2 earthquake, a total of four waves consisting of two waves each were selected from type I (large-scale plate boundary earthquake) and type II (large-scale inland earthquake). Concerning type II, the input waveform was multiplied by the reduction factor shown in the “Description” column in Table 3 to prevent the shear strain on the upper and lower rubber bearing from exceeding 200% during shaking at Case4.

Table 3 – Specifications of the input waveform

Seismic shaking level	Waveform name	Max acceleration [cm/sec ²]	Duration [sec]	Description
Level-1	L1-III	140	34	A waveform that is corrected by multiplying the similarity index (1/1.49) by the time axis of level-1 earthquake motion (III type ground) which has a high probability of occurring during the in-service period
Level-2	I-II-2	675	161	A waveform that is corrected by multiplying the similarity index (1/1.49) by the time axis of type I (II or III type ground) of a level-2 earthquake, which is assumed to be a plate boundary type earthquake
	I-III-3	691	161	
	II-II-2	404	34	A waveform that is corrected by multiplying the similarity index (1/1.49) by the time axis of a level-2 earthquake motion type II (II, III type ground) which is assumed to be an inland type earthquake, and in addition a waveform that is corrected by multiplying the reduced magnification (II-II-2:0.6, II-III-3:0.) by the acceleration
	II-III-3	495	34	

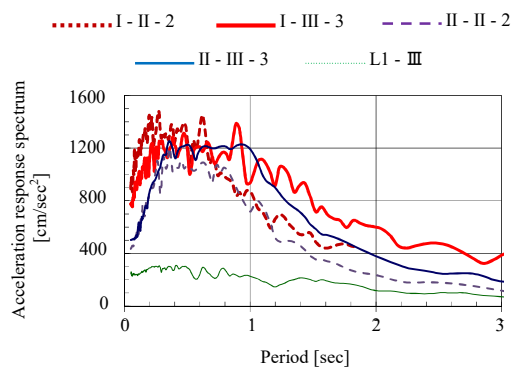


Fig. 7 – Spectrum of acceleration response of input waveform (the attenuation constant : 5%)



4. The result of shaking table test at level-1 earthquake

Regarding the time history waveform of the upper interlayer displacement obtained from a level-1 earthquake (L1-III type), Case 1, Case2 and Case4 were compared with each other, and the results shown in Fig. 8. From Fig. 8, concerning Case4 in which a DRF-damper is not installed, it was found that whereas an upper interlayer displacement of about 25 mm occurred, in Case2 in which a 200 kN DRF-damper is installed, the upper interlayer displacement is the maximum of 2 mm as same as Case1 in which corresponds to a fixed bearing condition. This value is extremely small. Consequently, it can be seen that the DRF-damper functions as a fixed member. Also, Fig. 9 shows the DRF-damper load versus displacement in Case2. From Fig. 9, it was found that the maximum value of the damper load during a level-1 earthquake was 140 kN ($\beta = 0.28$). It can thus be said that if the damper load is set higher than this value, the DRF-damper will function as a fixed member, without the damper sliding, during a level-1 earthquake. From the above, it could be verified that if the damper load is set to an appropriate value, the DRF-damper will function as a fixed member.

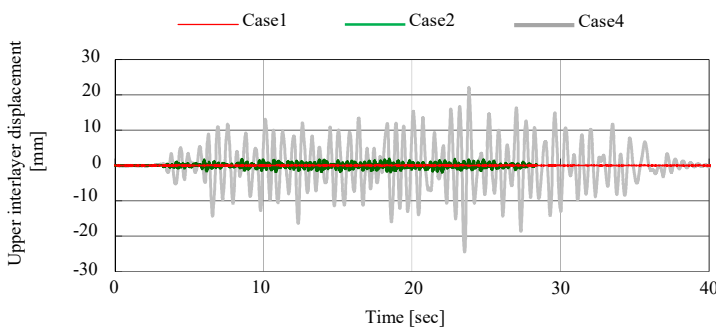


Fig. 8 – Time history waveform for upper interlayer displacement (L1-III)

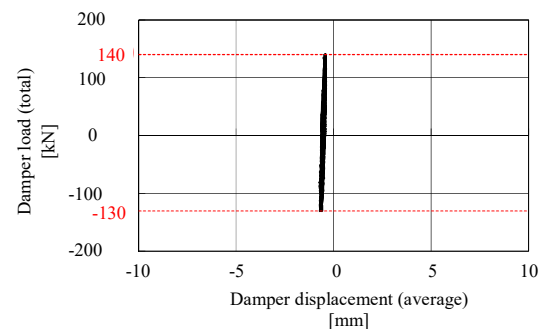
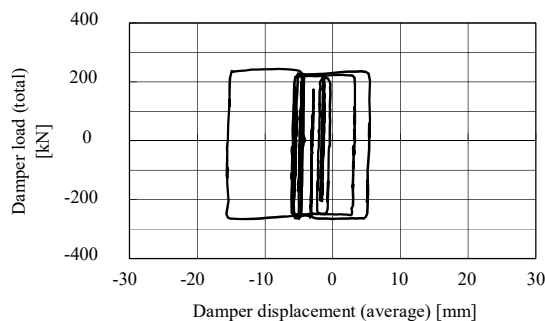


Fig. 9 – Load versus displacement of the DRF-damper shown in Case2

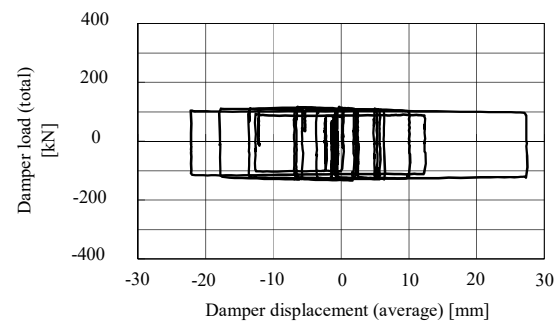
5. The result of shaking table test at level-2 earthquake

5.1 Behavior DRF-damper

The load versus displacement obtained during a level-2 earthquake (II-II-2) shaking is shown in Fig. 10. From Fig. 10, in both of Case2 (200 kN DRF-damper) and Case3 (100kN DRF-damper), there is a slight tendency for the damper load obtained shaking test to be higher than damper load were set. However, this figure indicates the stabilized rigid-plastic history characteristics.



(a) Case2 (200 kN DRF-damper)



(b) Case3 (100 kN DRF-damper)

Fig. 10 – Load versus displacement of DRF-damper during a level-2 earthquake (II-II-2) shaking



5.2 Result of reducing a response

The time history waveform of the lower interlayer displacement obtained from level-2 earthquake (I-II-2, II-II-2) shaking is shown in Fig. 11 comparing between Case1 and Case3. From Fig. 11, it can be seen that, compared to Case1 (before reinforcement), the maximum response value of the lower interlayer displacement of Case3 (after reinforcement) in which a 100 kN DRF-damper was installed fell to one half. A list of the maximum response values of the lower interlayer displacement for each shaking is shown in Table 4. From Table 4, it can be seen that the maximum response value of the lower interlayer displacement does not rely on the difference between each waveforms. Compared to Case1, for Case2 in which a 200 kN DRF-damper is installed, this value fell by about 30 to 40 %, and for Case3 in which a 100 kN DRF-damper is installed, it fell by about 40 to 60%. In case of Case4 which only a rubber bearing, the lower interlayer displacement occurred like that of Case1.

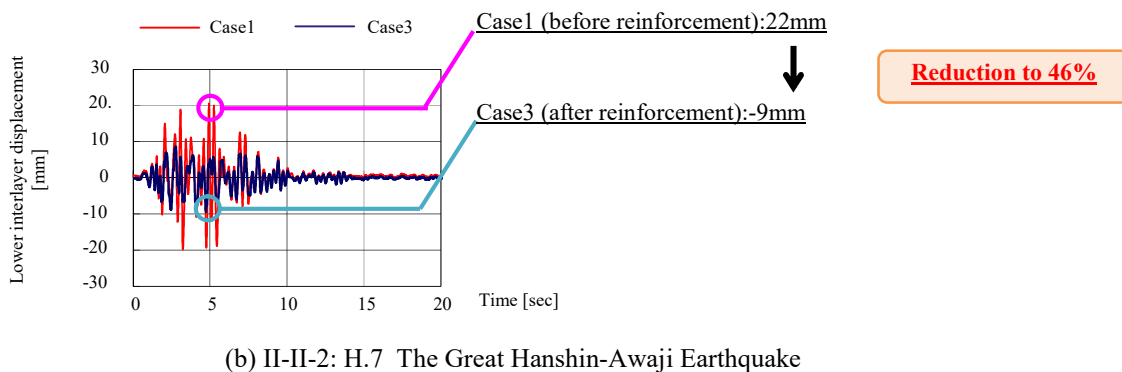
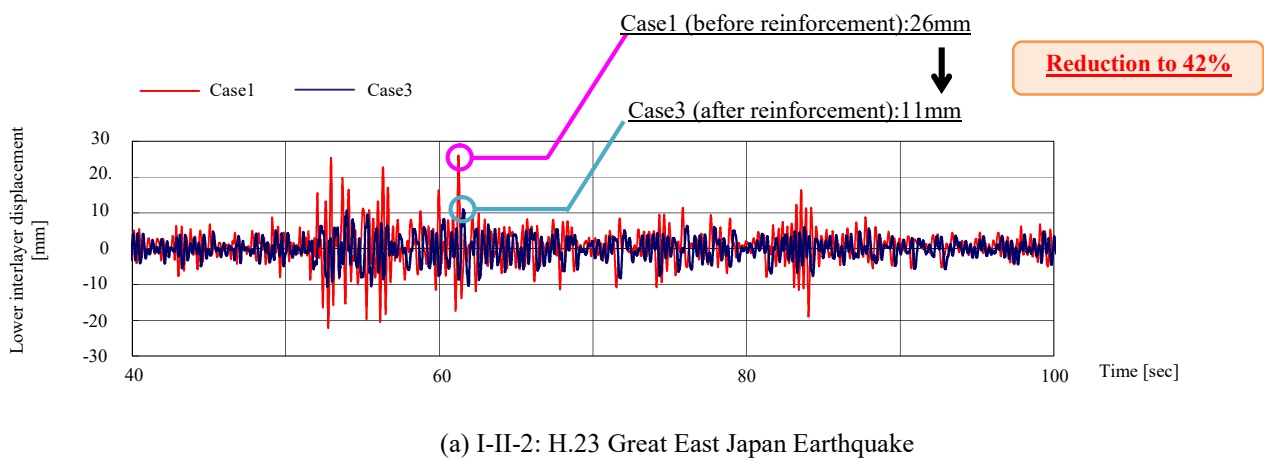


Fig. 11 – Time history waveform of the lower interlayer displacement

Table 4 – List of maximum response value of the lower interlayer displacement

Input waveform	Lower bearing displacement [mm]				Ratio of the lower level bearing displacement for each shaking case compared to Case1 [%]		
	Case1	Case2	Case3	Case4	$\frac{\text{Case2}}{\text{Case1}}$	$\frac{\text{Case3}}{\text{Case1}}$	$\frac{\text{Case4}}{\text{Case1}}$
	Before reinforcement	After reinforcement	After reinforcement	—			
	Fixed	Rubber bearing + 200 kN DRF-damper	Rubber bearing + 100 kN DRF-damper	Rubber bearing only			
I-II-2	26	15	11	19	59%	42%	73%
II-II-2	21	14	9	19	68%	46%	92%
I-III-3	20	15	12	22	75%	60%	111%
II-III-3	21	14	12	26	70%	60%	127%



5.3 Relationship between the damper load and the maximum response value

Figure 12 shows the transition of the maximum response value when the damper load was changed through Case1 to Case4, for each input waveform. Figure 12 (a) shows the upper interlayer displacement, and Fig. 12 (b) shows the lower interlayer displacement. The horizontal axis is the maximum damper load obtained for each shaking. The maximum damper load of Case1 was made the same as the upper maximum inertial force (upper mass \times maximum upper acceleration). First, from Fig. 12 (a), it can be seen that the maximum response to the upper interlayer displacement has fallen abruptly as a result of increasing the damper load. Also, it can be said that likewise regardless of the input waveform, because the secondary curve had been drawn, adjusting the damper load will enable the upper displacement to be controlled. Next, from Fig. 12 (b), regardless of the input waveform, if the damper load is increased, the maximum response value of the lower interlayer displacement will first decrease over the range between Case4 to Case3, and then increase over the range between Case3 and Case1. In other words, it can be seen that, over the range of $\beta = 0.2$ to 0.4, an optimum value of damper load that results in the minimum lower interlayer displacement exists. The existence of an optimum value has been examined by means of dynamic analyses according to References [3], [10], [11], etc., and that the results thereto agree well with this test results.

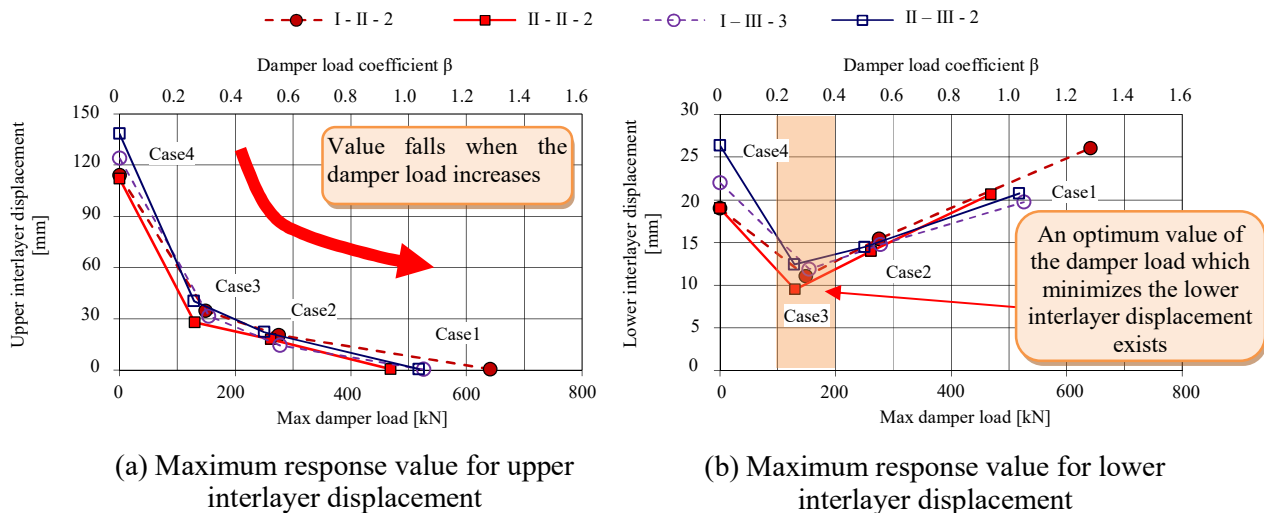


Fig. 12 – Transition of maximum response value when the damper reaction force is changed

5.4 Residual displacement of the upper interlayer displacement

Table 5 shows a list of the residual displacement values for the upper interlayer displacement. From Table 5 it can be seen that the maximum value of the residual displacement is about 5 mm, and even when it is multiplied by the scale ratio shown in Table 1, it is still only about 11 mm. In other words, it can be seen that if a DRF-damper is used in combination with a rubber bearing, the residual displacement can be suppressed.

Table 5 – List of residual displacement of the upper interlayer displacement

Input waveform	Residual displacement of upper interlayer displacement [mm]			
	Case1	Case2	Case3	Case4
	Fixed	Rubber bearing + 200 kN DRF-damper	Rubber bearing + 100 kN DRF-damper	Rubber bearing only
I-II-2	0.0	-5.4	-0.4	0.0
II-II-2	0.0	-1.6	1.7	0.1
I-III-3	0.0	-0.4	-1.7	-0.1
II-III-3	0.0	-0.6	-2.1	0.9



6. Conclusion

This paper showed we made a bridge model which modeled RC single column bridge piers and installed the DRF-dampers and the result of the shaking table test reproducing the dynamic behavior at the time of earthquake. The knowledge acquired is as follows.

- 1) As a result of shaking by level-1 earthquake, it was found that the DRF-damper functioned as a fixed member without sliding.
- 2) As a result of shaking by level-2 earthquake, it was found that by installing a DRF-damper for seismic reinforcement, the lower interlayer displacement corresponding to the deformation (damage) of the lower structure falls by a maximum of 60 % compared before reinforcement.
- 3) As a result of shaking by changing the damper load coefficient β (value of the damper load divided by the total weight of the upper level) in four steps at the level-2 earthquake, it can be seen that, over the range of $\beta = 0.2$ to 0.4 , an optimum value of β that results in the minimum lower interlayer displacement exists. This corresponds well with the results of analysis performed during previous research.

7. Acknowledgements

This research constitutes part of the research related to “Research concerning improved technology for seismic resistance of existing bridges,” which is joint research performed by Metropolitan Expressway Company Limited and Asunaro Aoki Construction Co., Ltd. Also, the shaking table test was carried out at the end of January, 2016 using a large 3-dimensional shaking table possessed by Public Works Research Institute. Here the authors wish to thank the parties concerned for their detailed guidance concerning the coordination of the planning and execution of the test, and also arranging the results thereto.

8. References

- [1] H. Miyamoto, T. Matsuda, H. Uno and M. Fujimoto (2013): “Study on Applicability of Nonlinear Response Spectrum to Bridge Seismic Design with Vibration Control Damper”, A collection of papers published by the Japan Society of Civil Engineers A1 (Structure and Earthquake Engineering), Vol.69, No.4, 592-600(in Japanese)
- [2] M. Hada, K. Kuraji, Y. Migitaka and S. Ushijima (2019): “DEVELOPMENT OF DIE AND ROD FRICTION DAMPER FOR SEISMIC RETROFITTING ON ROAD BRIDGES”, A collection of papers published by the Japan Society of Civil Engineers A1 (Structure and Earthquake Engineering), Vol.75, No.2, 95-110(in Japanese)
- [3] M. Hada, K. Kuraji, Y. Migitaka and S. Ushijima (2016): “Development of a Die and Rod Friction Damper Used for Improving the Seismic Resistance of Existing Bridge”, Proceedings of the Japan Concrete Institute, Vol.38, No.2, 1003-1008(in Japanese)
- [4] M. Hada, A. Wada, S. Kubota and S. Ushijima (2017): “DEVELOPMENT OF DIE AND ROD FRICTION DAMPER FOR SEISMIC RETROFITTING ON ROAD BRIDGES”, 15th REAAA Conference & IRF Global Road Summit, Bari-Indonesia
- [5] A. Yamasaki, M. Hada, H. Kimura, S. Ushijima, K. Kuraji, T. Matsubara and S. Kubota (2018): “Development of “Die and Rod Type Friction Damper” with a Capacity of 1,200kN Level”, Proceedings of the 73th Annual Meeting of Japan Society of Civil Engineers, 631-632(in Japanese)
- [6] M. Hada, K. Kuraji, Y. Migitaka and S. Ushijima (2017): “Shaking Table Test of Bridge Model using Die and Rod Type Friction Damper”, Proceedings of the Japan Concrete Institute, Vol.39, No.2, 859-864(in Japanese)
- [7] M. Hada, K. Fujimoto, K. Kobayashi, S. Ushijima, K. Kuraji and A. Wada (2018): “Shaking Table Test of a Bridge Model Installed Friction Dampers”, Proceedings of The 15th Japan Earthquake Engineering Symposium, 3389-3396(in Japanese)
- [8] K. Kitajima, H. Onishi, M. Nakanishi and H. Adachi (1999): “A Study on Friction Damper for Response-Control Retrofit of Existing R/C Buildings”, Proceedings of the Japan Concrete Institute, Vol.21, No.1, 385-390(in Japanese)



- [9] Japan Road Association (2012): Specifications for highway bridges part V Seismic Design (in Japanese)
- [10] A. Takeda and K. Tanaka (2011): “Shaking Table Tests of Bridge Models with Friction Dampers”, Proceedings of the Japan Concrete Institute A1 (structure and earthquake engineering), Vol.67, No.3, 628-643 (in Japanese)
- [11] A. Yamasaki, M. Hada, S. Ushijima, T. Matsubara and K. Yamamoto (2019): “Study of the Effect of Seismic Control of Road Bridge Installed “Friction Dampers””, Proceedings of the 14th Annual Meeting of Japan Association for Earthquake Engineering, P2-29 (in Japanese)